Simulation and design of a Long Period Grating Fiber Sensor system for detection of Klebsiella pneumoniae infestation of water

SORIN MICLOS[a], DAN SAVASTRU[a], ROXANA SAVASTRU[a], FLORINA-GIANINA ELFARRA[b], ION LANCRANJAN[a,*]
[a]*National Institute of R&D for Optoelectronics - INOE 2000, 409 Atomiștilor St., Măgurele, Ilfov, RO-077125, Romania*
[b]*"Sfântul Ion" Emergency Clinical Hospital, 13 Vitan-Bârzești Street, Bucharest, Romania*

This paper is dedicated to simulation and design of a long period grating fiber sensor setup for detection of pathogen bacteria *Klebsiella pneumoniae* infestation of water. The results obtained using a simulation model which generates information on the biochemistry of the investigated micro-organism and the long period grating fiber sensor characteristics are presented. The main purpose of the simulation is to accomplish an optimal long period grating fiber sensor setup for an improved design of a portable device for real-time detection of a nosocomial infection source such as *Klebsiella pneumoniae*.

(Received December 05, 2018; accepted February 12, 2019)

Keywords: Klebsiella pneumoniae, Refractive index measurement, Biochemical sensing

1. Introduction

Among the micro-organisms of Enterobacteriaceae class in which there are found important pathogen agents causing both nosocomial and community-acquired infections there are included two very similar bacteria whose real-time detection, in minutes, is under intense investigation: *Escherichia coli* (*E. coli*) and *Klebsiella pneumoniae* (*K. pneumoniae*) [1-10]. During the last fifty years important researches were performed concerning these two bacteria, especially regarding a medical issue of great concern: the emergence of their multi-antibiotic resistance [2-10]. Their resistance to broad-spectrum cephalosporins which is typically associated with the acquisition of mobile genetic elements such as plasmids and transposons is intensively investigated [2]. Such plasmids contain genes that encode for extended-spectrum -lactamases (ESBLs) but may also contain other resistance genes as well. For most Enterobacteriaceae, their resistance to carbapenems has been uncommon [3-8]. However, according to the data reported in literature, K. pneumoniae has acquired a novel resistance mechanism to carbapenems, mechanism known as *K. pneumoniae* carbapenemase (KPC) -lactamase [8].

Commonly, *K. pneumoniae* infections are observed mostly in people with a weakened immune system [2-10]. Most often, *K. pneumoniae* illness affects middle-aged and older men with debilitating diseases who also have impaired respiratory host defenses, diabetes, alcoholism, malignancy, liver disease, chronic obstructive pulmonary diseases, glucocorticoid therapy, renal failure, and certain occupational exposures, for example papermill workers. Many of these infections are observed when a person is in the hospital for some other reason such as a nosocomial infection. As in the *E. coli* case, the feces are the most significant source of patient infection, the contact with contaminated instruments being also an important infection source. The most common condition caused by *K. pneumoniae* bacteria outside the hospital is pneumonia, typically in the form of bronchopneumonia and bronchitis. These patients have an increased tendency to develop lung abscess, cavitation, empyema, and pleural adhesions. It has a death rate around 50 %, even under anti-microbial therapy. Besides pneumonia, *K. pneumoniae* can also cause infections in the urinary tract, lower biliary tract, and surgical wound sites. The range of clinical diseases includes pneumonia, thrombophlebitis, urinary tract infection, cholecystitis, diarrhea, upper respiratory tract infection, wound infection, osteomyelitis, meningitis, bacteremia, and septicemia. For patients with an invasive device in their bodies, contamination of the device becomes a risk. For instance, neonatal ward devices, respiratory support equipment, and urinary catheters expose the patients at an increased risk. Also, the use of antibiotics can be a factor that increases the risk of nosocomial infection with *K. pneumoniae* bacteria. Sepsis and septic shock can follow entry of the bacteria into the blood.

As a conclusion of all these previously mentioned remarks an easy to use, portable small size system for early detection of *K. pneumoniae* is necessary. A *K. pneumoniae* detection device using biochemical fiber optic

sensors such as Long Period Grating Fiber Sensor (LPGFS) appears as the most suitable for this purpose including continuous monitoring if necessary [1, 11-31]. The basic principle of LPGFS operation for *K. pneumoniae* detection in water consists in measuring the refractive index variations of the optical fiber ambient medium when the bacteria is infesting the water compared to pure, non-infested water [1, 11-31]. The design of such LPGFS devices, manufactured into single mode (SM) optical fiber, relies to a large extent on applying simulation techniques mainly for light guided propagation through optical fiber core and its scattering on the grating pitch [1, 28-36]. An important task to be accomplished by the developed simulation models consists in improvement of conception, design, fabrication, and characterization of optical fiber configurations with enhanced evanescent field interaction with the ambient [28-44]. In subsidiary, a special care is paid to new design approaches applied in order to overcome cross sensitivity effects between several parameters to be measured, especially the temperature [23-43]. Advanced LPGFS interrogation schemes, e.g. conception, implementation, and characterization with virtual instrumentation for interferometric sensors, represent other important tasks of the simulations [4-9].

As a starting point is the observation that the pathogen bacteria and other micro-organisms are living entities which interact with the milieu by exchanging energy and different chemical compounds. The developed simulation model presented in the paper has two components. One component is defined on computational biochemistry basis and refers to the quantitative definition of functional cycle of bacteria or other type of micro-organisms under investigation starting from their genetic code [6-10]. In this first model, the concentrations of enzymes, polysaccharides, lipids, and other compounds generated by the investigated micro-organisms were determined. The second component of the simulation model has the task to optimize the constitutive characteristics of one or two LPGFS used simply as it is or in interferometric Mach-Zehnder in-fiber setups such as cascade or twins' arrangements [6-24]. The second simulation model has an important feature: it is developed for the case of an ambient milieu of the LPGFS with a refractive index higher than that of the fiber cladding.

2. Theory

2.1. Simulation model of *K. pneumoniae*

Brief remarks concerning *K. pneumoniae*. *K. pneumoniae* is a Gram-negative, alike *E. coli*, (but non-motile, in opposition to *E. coli*), encapsulated, lactose fermenting, facultative anaerobic, rod-shaped with rounded, almost semi-spherical end bacterium. *K. pneumoniae* and *E. coli* have almost the same dimensions, 3-4 μm length and 0.75-1 μm diameter. *K. pneumoniae* and E. coli have dimensions comparable with the wavelengths of the light with which the LPGFS operates. *K. pneumoniae* can be found in the human or animal normal flora of the mouth, skin, and intestines [3-10]. If inhaled, *K. pneumoniae* can cause destructive changes to human or animal lungs, specifically to the alveoli, resulting in bloody sputum. In the clinical setting, it is the most significant member of the *Klebsiella* genus of the *Enterobacteriaceae*. In recent years, *K. pneumoniae* have become the most important pathogen in nosocomial infections. *K. pneumoniae* naturally occurs in soil and can fix nitrogen in anaerobic conditions [2-10]. As a free-living diazotroph, its nitrogen-fixation system has been much-studied, being of agricultural interest, as *K. pneumoniae* has been demonstrated to increase crop yields in agricultural conditions [7-10]. *K. pneumoniae* ranks second to *E. coli* for urinary tract infections in older people. It is also an opportunistic pathogen for patients with chronic pulmonary disease, enteric pathogenicity, nasal mucosa atrophy, and rhino-scleroma. The epidemiology of resistance is complex since it is believed that it combines the spread of certain bacterial strains with the independent spread of plasmids. On the other hand, studies show that transmission of the bacterium is associated with the spread of a single successful clone [4-6, 10].

Brief remarks concerning the *K. pneumoniae* biochemistry simulation model. As mentioned in [1], like in the *E. coli* case, a life cycle biochemistry simulation model was developed for *K. pneumoniae* based on a commercial software package, MATLAB 8.9 [1, 6 -10]. In the structure of the bulk of the developed computational biochemistry simulation model enters 274 routines and sub-routines with 55,545 lines of program code which allows evaluation of an optimal path from several known possible chemical reactions involving the biochemical compounds previously known as possible being in the composition of the investigated *K. pneumoniae* bacterium strain. For a given set of ambient conditions, from the computational biochemistry simulation model of an investigated *K. pneumoniae* bacterium the concentrations of enzymes, polysaccharides, lipids, fatty acids, proteins and other biochemical compounds generated/interchanged with the ambient by the micro-organisms under investigation were determined. Each *K. pneumoniae* bacterium strain biochemical compound has optical (e.g. refractive index) and spectroscopically characteristic parameters which allows accurate identification using optical detection devices such as LPGFS.

As mentioned in [1], there are five infrared spectral windows which were considered in connection with the developed computational biochemistry simulation model. The first window, situated between 3,000 and 2,800 cm^{-1}, contains C-H stretching vibrations of CH, CH_2 and CH_3 in the functional groups of membrane fatty acids and of

amino acid side-chains. The second window, situated between 1,800 and 1,500 cm^{-1}, contains C=O stretching vibrations of amides linked to proteins, N-H deformation of amides linked to proteins, >C=O stretching vibrations of the ester groups in lipids and >C=O, >C=N, >C=C< stretching of the DNA or RNA bases. The third window, situated between 1,500 and 1,200 cm^{-1}, contains $>CH_2$ and $-CH_3$ bending modes. The fourth window, situated between 1,200 and 900 cm^{-1}, contains symmetric stretching vibrations of PO^{-2} groups in nucleic acids C-O-C and C-O-P stretching of carbohydrates and poly-saccharides in the cell membrane. The fifth window, situated between 900 and 700 cm^{-1}, contains aromatic ring vibrations of aromatic amino acids [5-9]. The life cycle of the *K. pneumoniae* bacterium simulation model, considering its genetic code, is presented schematically in [1] as applied in the case of *E. coli* infesting milk. The life cycle of the *K. pneumoniae* bacterium simulation model involves 1,658 bio-chemical compounds which participate at 2,257 possible chemical reactions [3-6].

2.2. LPGFS simulation model

It is necessary to mention that in [1] the detailed comments concerning the LPGFS simulation model are presented. Nevertheless, in the followings the main ideas of how is operated the simulation model of *K. pneumoniae* infestation in water are briefly presented. In Fig. 1 the structure of a detection setup used for detection of *K. pneumoniae* infesting water is schematically presented [1]. The sensing component of this setup is the LPGFS whose outer surface is in direct contact with the water which is possible infested with *K. pneumoniae* over the length *L* of the fiber optic zone where the Long Period Grating (LPG) is located. It is manufactured into a single mode (SM) optical fiber by inducing a permanent spatial modulation of the light propagation characteristics over a length *L*.

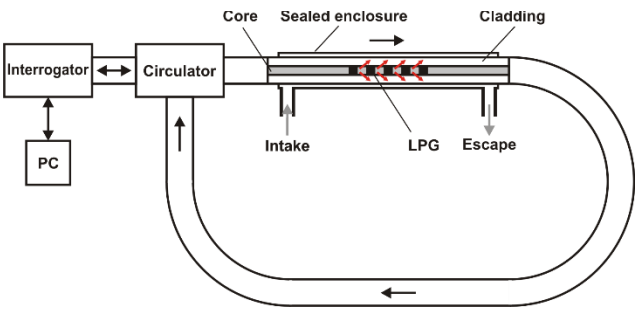

Fig. 1. Schematic representation of a LPGFS and its operation mode [1]

Another main consideration refers to Eqs. (1) and (2) which define the Bragg resonance condition of λ^i, for the investigated LPGFS [1, 10-21, 31-44]. λ^i defines the peaks of the absorption bands corresponding to the Bragg resonance condition which appear in the LPG transmission spectrum [1, 10-21, 31-44]. λ^i are defined as

$$\lambda^i = \left(n_{eff} - n^i_{clad}\right) \cdot \Lambda \tag{1}$$

or

$$\lambda^i = \left(n_{eff} - n^i_{clad}\right)\Lambda + \left(\kappa_{c-c} - \kappa_{cl-cl}\right) \tag{2}$$

where λ^i are the absorption bands maxima wavelengths, n_{eff} and n^i_{clad} are the effective values of the core and cladding refractive index, Λ is the period of the LPG, κ_{c-c} and κ_{cl-cl} are the self-coupling coefficients of the core mode and the cladding mode, respectively. κ_{c-c}, κ_{cl-cl}, n_{eff} and n^i_{clad} which cannot be defined analytically, but as numerical solutions to equations deduced from electromagnetic theory, depend implicitly on the LPGFS ambient refractive index, n_{am}. Eq. (2) is a more accurate form of Eq. (1) by adding a term considering κ_{c-c} and κ_{cl-cl}. Eq. (2) expresses mathematically that a small fraction of the cladding mode field, the evanescent field, travels outside the optical fiber, into the ambient milieu interacting with it, changing n^i_{clad} and λ^i.

The LPGFS sensing principle relies on observing the λ^i changes induced by any n_{am} variation. λ^i changes are observed as spectral shifts of the absorption bands characteristic of the investigated LPGFS [1, 10-21, 31-44]. In the case of detecting *K. pneumoniae* infestation in water, the n_{am} variation is induced by the biochemical compounds which are exchanged by the bacteria with water. It is a thin line between the domains in which Eq. (1) or Eq. (2) is enough accurate to be used one instead of the other. It can be justified theoretically that the sensitivity to ambient refractive index of LPGFSs, more precisely of the LPG, can be increased up to 2,500 nm/r.i.u. (r.i.u. means refractive index unit) which is enough for *K. pneumoniae* detection.

3. Simulation results

As detailed presented in [1], the simulation of a LPGFS device which detects *K. pneumoniae* infestation in water is performed in two main stages each having several sub-stages with the final task to obtain the spectral shift of a characteristic absorption band induced in the LPGFS transmission spectrum. The first stage consists of defining the LPGFS spectral parameters [1]. The second stage consists in obtaining spectral information concerning the *K. pneumoniae* specific biochemical compounds and their

spectroscopic parameters, mainly in connection with the five spectral windows specified in Section 2 [1].

Both geometrical and refractive index parameters of the LPGFS are identical to the ones defined in [1], which correspond to Corning SMF 28e and Fibercore SMF 750 optical fibers. The LPGFS parameters are: core radius = 2.8 μm, core refractive index = 1.4589, cladding radius = 62.5 μm, cladding refractive index = 1.4557 and cut-off wavelength = 650 nm [25-31]. The issue concerning the dispersion of core refractive index, presented in [1], was re-analyzed. The variation of core refractive index over the investigated light wavelength range (700-1,700 nm) is extremely low. Therefore the simulation procedure run considering the core refractive index dispersion did not give any significant different result compared to the constant index case. This is the reason why the simulation results were obtained with the previously mentioned core refractive index of 1.4589 [1].

As presented in [1], the next step of the simulation procedure consists in defining the inputs of Eqs. (1) and (2), i.e. the effective refractive index values of the core and cladding propagating modes, n_{eff} and n_{clad}^{i} obtained by numerically solving the equations of light propagation through the optical fiber. The additional inputs of Eq. (2), $\kappa_{c\text{-}c}$ and $\kappa_{cl\text{-}cl}$, are obtained using an approximative relation deduced from [18]. The inputs of Eqs. (1) and (2) are calculated using a three-layers model of the optical fiber: the optical fiber core and cladding are the first two layers and the ambient is the third. In Fig. 2, the variation of core effective refractive index (n_{eff}) vs. light wavelength is presented. For the investigated LPGFS, the simulation procedure indicates that there are 457 possible cladding propagation modes. In Fig. 3, the variations versus light wavelength of the effective refractive index corresponding to the first nine possible cladding propagation modes are presented. The simulated n_{eff} and n_{clad}^{i} are used to define the characteristic phase matching curves (PMC) of the investigated LPGFS. It must be observed that for a given LPGFS, the PMC are a set of parametric bidimensional curves, each of them representing a light mode of propagation through the optical fiber. Each point of such a curve represents a pair of light wavelength and grating period (Λ_{LPG}) satisfying the Bragg resonance condition. For a fixed Λ_{LPG} the points on the PMC set define the wavelengths λ^{i} where the peaks of the absorption bands in the LPGFS transmission spectrum are located.

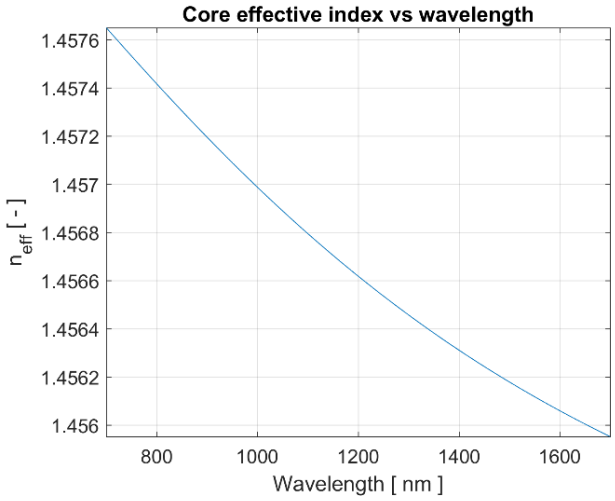

Fig. 2. Variation of the core effective refractive index n_{eff} vs. wavelength

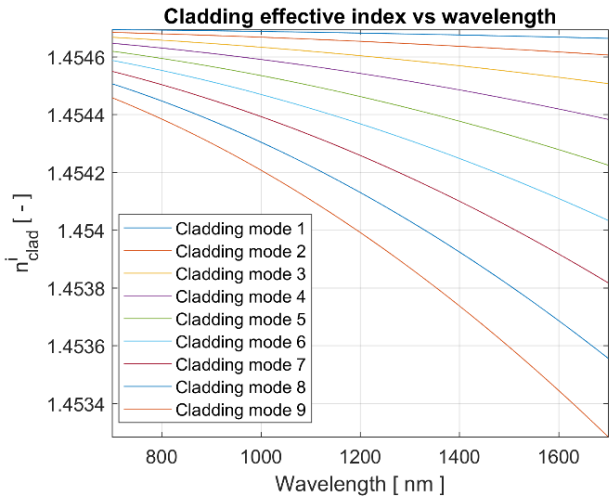

Fig. 3. Variations of the cladding effective refractive index n_{clad}^{i} vs wavelength for the first nine cladding modes

In Figs 4 - 7 the simulation results obtained for PMC using Eqs. (1) and (2) are presented. In Fig. 4 (using Eq. (1)) and in Fig. 5 (using Eq. (2)) PMC as Λ_{LPG} vs. wavelength parametric curves are presented. In Fig. 6 (using Eq. (1)) and in Fig. 7 (using Eq. (2)) PMC as wavelength vs. Λ_{LPG} parametric curves are presented. For both Eqs. (1) and (2), the simulation results for PMC are presented in the two alternative variants of analyzing PMC as parametric curves, whichever is preferred. The comments referring at LPGFS operation mode become clear after the significance of the PMC is analyzed. In each of the plots, presented in Figs. 4 - 7 the intersection point of a horizontal or vertical line (i.e. corresponding to a given value of Λ_{LPG} or light wavelength) with the phase matching curves defines the peaks λ^{i} of absorption bands appearing in the LPGFS transmission spectrum.

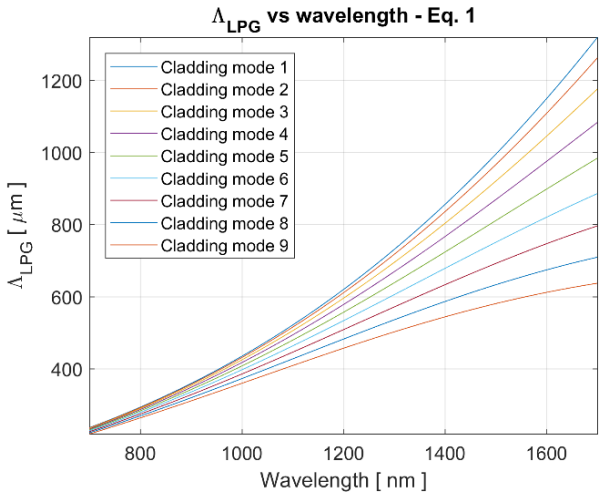

Fig. 4. The PMC obtained using Eq. (1) represented as Λ_{LPG} vs. wavelength for the first nine cladding light modes

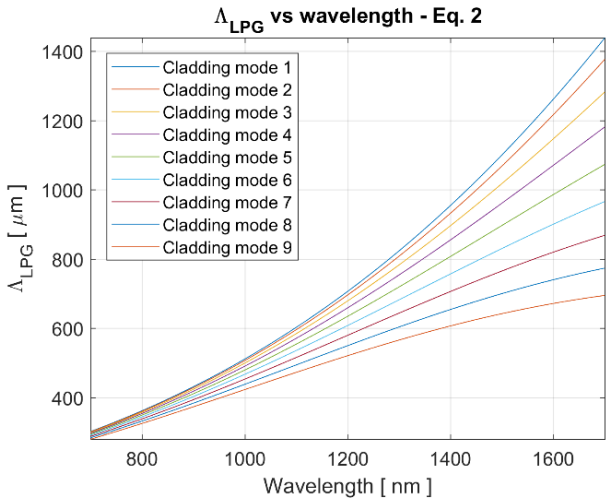

Fig. 5. The PMC obtained using Eq. (2) represented as Λ_{LPG} vs. wavelength for the first nine cladding light modes

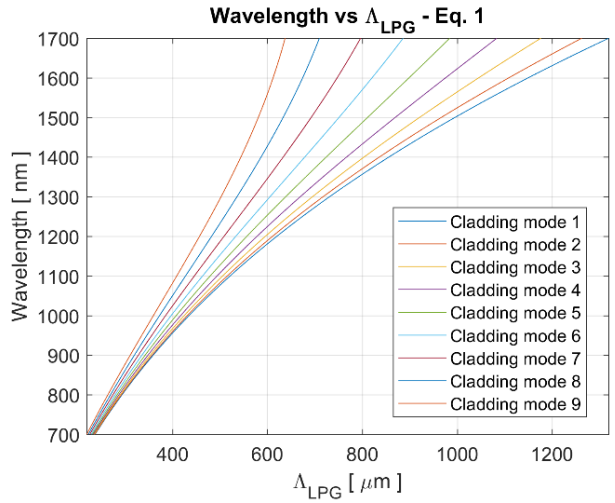

Fig. 6. The PMC obtained using Eq. (1) represented as wavelength vs. Λ_{LPG} for the first nine cladding light modes

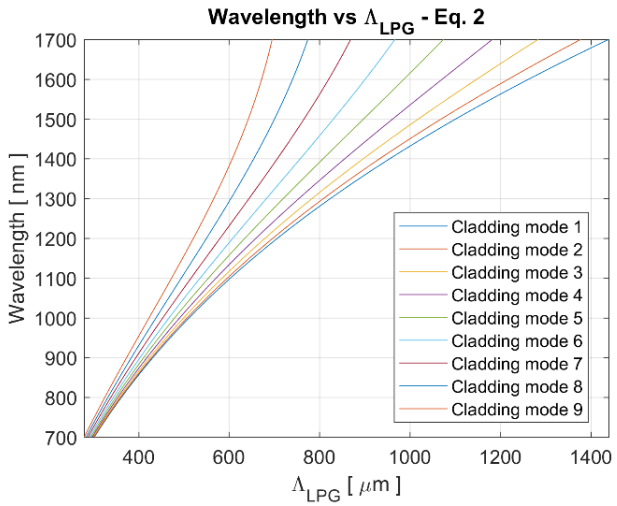

Fig. 7. The PMC obtained using Eq. (2) represented as wavelength vs. Λ_{LPG} for the first nine cladding light modes

It appears that the following procedure can be applied in the case of *E. coli* infesting milk [1] for detection of *K. pneumoniae* infesting water using LPGFS. For a given Λ_{LPG}, on the PMC set is chosen a λ^i situated in the vicinity, up to 10-20 nm in spectral range, of a peak wavelength corresponding to a maximum absorption band of the transmission spectrum of a biochemical compound characteristic of *K. pneumoniae*. For increasing the certainty of a *K. pneumoniae* strain identification using LPGFS, several such wavelengths must be chosen, at least one for each of the spectral windows previously mentioned in Section 2, preferable corresponding to different biochemical compounds uniquely characteristic of the *K. pneumoniae* strain.

K. pneumoniae infestation induces spectral shifts of λ^i compared to the transmission spectrum of LPGFS placed in non-infested water. In Fig. 8, the simulation results obtained for such a spectral shift of λ^i caused by *K. pneumoniae* infestation in water are presented. An absorption band specific to a *K. pneumoniae* biochemical compound of lipopolysaccharide type was investigated. The maximum absorption band of the K. pneumoniae biochemical compound is situated at ~1,520 nm. The value of λ^i for Bragg resonance condition in non-infested water is 1,530 nm with a 104.76 nm full width half measure bandwidth (FWHM). A slight increase of ambient refractive index was considered to cause a spectral shift of λ^i down to 1,515.5 nm with FWHM increased to 109.26 nm. It was roughly estimated a *K. pneumoniae* concentration of 1.25×10^8 cfu/mL (cfu - colony forming unit for quantification of pathogen bacteria concentration).

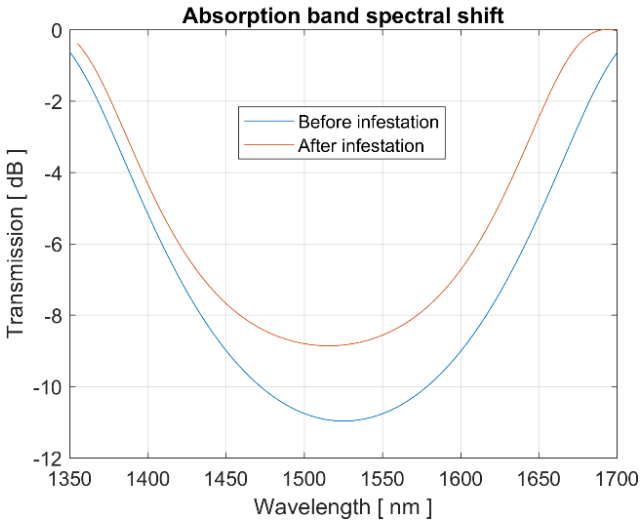

Fig. 8. The simulated spectral shift of LPGFS absorption band induced by the K. pneumoniae infestation of water

4. Conclusions

The simulation results presented in this paper open a new design method of LPGFS dedicated to detection of *K. pneumoniae* infestation of water.

Based on the computational biochemistry simulation model, a LPGFS was designed to operate with maximum sensitivity in a spectral domain in which *K. pneumoniae* biochemical compounds are present and have a significant spectral signature.

A *K. pneumoniae* concentration of 1.25×10^{8} cfu/mL produced a spectral shift of absorption band maximum (situated at wavelength 1,530 nm) with a 104.76 nm FWHM in the case of non-infested water to an absorption band maximum (situated at wavelength 1,515.5 nm) with FWHM increased to 109.26 nm in the case of the infested water. All these modifications can be easily measured using a commercial fiber interrogator, putting in evidence the presence of the bacterium. The results of this study provide a useful tool to design a very sensitive *K. pneumoniae* detector. The accuracy of the detection method can be largely improved by imposing an increased number of specific spectral identification points.

Acknowledgments

This work was supported by the MANUNET grant MNET17/NMCS0042 and by the Core Program project no. PN 18 28.01.01.

References

[1] D. Savastru, S. Miclos, R. Savastru, I. Lancranjan, J. Optoelectron. Adv. M. **20**(11-12), 610 (2018).
[2] Z. A. Memish, A. Zumla, R. F. Alhakeem, A. Assiri, A. Turkestani et al., Lancet **383** (9934), 2073 (2014).
[3] S. H. Lau, J. Cheesborough, M. E. Kaufmann, N. Woodford, A. R. Dodgson et al., Clin. Microbiol. Infect. **16**, 232 (2010).
[4] S. H. Lau, M. E. Kaufmann, D. M. Livermore, N. W. Geraldine, A. Willshaw et al., J. Antimicrob. Chemother. **62**(6), 1241 (2008).
[5] M. T. Nuesch-Inderbinen, H. Hachler, F. H. Kayser, Eur. J. Clin. Microbiol. Infect. Dis. **15**(5), 398 (1996).
[6] G. Peirano, J. D. Pitout, Int. J. Antimicrob. Agents **35**, 316 (2008).
[7] J. D. Pitout, Drugs **70**(3), 313 (2010).
[8] J. D. Pitout, Expert Rev. Anti Infect. Ther. **6**(5), 657 (2008).
[9] J. D. Pitout, L. Campbell, D. L. Church, P. W. Wang et al., J. Clin. Microbiol. **47**(4) 1212 (2009).
[10] S. W. James, R. P. Tatam, Meas. Sci. Technol. **14** (5), R49 (2003).
[11] T. Erdogan, J. Opt. Soc. Am. A **14**(8), 1760 (1997).
[12] T. Erdogan, J. Lightwave Technol. **15**(8), 1277 (1997).
[13] C. S. Cheung, S. M. Topliss, S. W. James, R. P. Tatam, J. Opt. Soc. Am. B **25**(6), 897 (2008).
[14] J. M. Lopez-Higuera, L. R. Cobo, J. Lightwave Technol. **29**(4), 587 (2011).
[15] J. F. Akki, A. S. Lalasangi, P. U. Raika, T. Srinivas, L. S. Laxmeshwar, U. S. Raikar, IOSR-JAP **4**(3), 41 (2013).
[16] Y. Koyamada, IEEE Photonic. Tech. L. **13**(4), 308 (2001).
[17] S. Kher, S. Chaubey, J. Kishore, S. M. Oak, IEEE Sens. J. **13**(11), 4482 (2013).
[18] R. Kashyap, "Fiber Bragg Gratings", Academic Press, 2009.
[19] P. Biswas, N. Basumallick, S. Bandyopadhyay, K. Dasgupta, A. Ghosh, S. Bandyopadhyay, IEEE Sens. J. **15**(2), 1240 (2015).
[20] X. Lan, Q. Han, J. Huang, H. Wang, Z. Gao et al., Sens. Actuators B Chem. **177**, 1149 (2013).
[21] X. Lan, Q. Han, T. Wei, J. Huang, H. Xiao, IEEE Photonic. Tech. L. **23**(22), 1664 (2011).
[22] S. Kher, S. Chaubey, R. Kashyap, S. M. Oak, IEEE Photonic. Tech. L. **24**(9), 742 (2012).
[23] V. Mishra, S. C. Jain, N. Singh, G. C. Poddar, P. Kapur, Indian J. Pure Ap. Phy. **46**, 106 (2008).
[24] A. Iadicicco, D. Paladino, P. Pilla, S. Campopiano, A. Cutolo, A. Cusano, Ch. 14: "Long Period Gratings in New Generation Optical Fibers". In: M. Yasin, S. W. Harun, H. Arof, Eds., "Recent Progress in Optical Fiber Research", InTech. 291 (2012).
[25] F. Chiavaioli, P. Biswas, C. Trono, S. Bandyopadhyay, A. Giannetti et al. Biosens Bioelectron. **60**, 305 (2014).
[26] R. Garg, S. M. Tripathi, K. Thyagarajan, W. J. Bock, Sens. Actuators B Chem. **176**, 1121 (2013).
[27] T. Allsop, K. Kalli, K. Zhou, Y. Lai, G. Smith et al., Opt. Commun. **281**(20), 5092 (2008).
[28] J. Kanka, Proc. SPIE **8426**, 34 (2012).
[29] J. Kanka, Sens. Actuators B Chem. **182**, 16 (2013).
[30] X. Shu, X. Zhu, Q. Wang, S. Jiang, W. Shi, Z. Huang, Electron. Lett. **35**(8), 649 (1999).

[31] M. Smietana, M. Koba, P. Mikulic, W. J. Bock, Meas. Sci. Technol. **25**(11), Article ID: 114001 (2014).
[32] S. Korposh, S. James, R. Tatam, S. W. Lee, Chapter 4: "Optical Fiber Long-Period Gratings Functionalised with Nano-Assembled Thin Films: Approaches to Chemical Sensing", In: C. Cuadrado-Laborde, Ed., "Current Trends in Short- and Long-Period Fiber Gratings", InTech. 63-86 (2013).
[33] D. Savastru, S. Miclos, R. Savastru, I. Lancranjan, Proc. SPIE **9517**, 95172A (2015).
[34] S. Miclos, D. Savastru, R. Savastru, I. Lancranjan, Compos. Struct. **183**(SI), 521 (2018).
[35] D. Savastru, S. Miclos, R. Savastru, I. Lancranjan, Compos. Struct. **183**(SI), 682 (2018).
[36] K. O. Hill, B. Malo, F. Bilodeau, D. C. Johnson, Annu. Rev. Mater. Sci. **23**, 125 (1993).
[37] S. Miclos, D. Savastru, I. Lancranjan, Rom. Rep. Phys. **62**(3), 519 (2010).
[38] I. Lancranjan, S. Miclos, D. Savastru, J. Optoelectron. Adv. M. **12**(8), 1636 (2010).
[39] I. Lancranjan, S. Miclos, D. Savastru, A. Popescu, J. Optoelectron. Adv. M. **12**(12), 2456 (2010).
[40] R. Savastru, I. Lancranjan, D. Savastru, S. Miclos, Proc. SPIE **8882**, 88820Y (2013).
[41] S. Miclos, D. Savastru, R. Savastru, I. Lancranjan, Proc. SPIE **9517**, 95172B (2015).
[42] D. Savastru, S. Miclos, R. Savastru, I. Lancranjan, Rom. Rep. Phys. **67**(4), 1586 (2015).
[43] R. Q. Lv, T. M. Zhou, L. B. Zhang, H. J. Peng, Y. N. Zhang, Optoelectron. Adv. Mat. **11**(11-12), 633 (2017).
[44] D. Liu, G. Humbert, Y. Liu, D. Zhao, Optoelectron. Adv. Mat. **11**(5-6), 289 (2017).

*Corresponding author: ion.lancranjan@inoe.ro